

Dear author,

Please note that changes made in the online proofing system will be added to the article before publication but are not reflected in this PDF.

We also ask that this file not be used for submitting corrections.

# Q2 Topographic bone thickness maps to evaluate the intuitive placement of titanium miniplates for nasal prostheses

K. Zaoui<sup>1</sup>, A. Jung<sup>1</sup>, W. Wimmer<sup>2,3</sup>, M. Engel<sup>4</sup>, M. A. Möhlenbruch<sup>5</sup>, P. A. Federspil<sup>1</sup> Q3

<sup>1</sup>Department of Otorhinolaryngology, University Hospital Heidelberg, Germany; <sup>2</sup>Hearing Research Laboratory, ARTORG Center for Biomedical Engineering Research, University of Bern, Switzerland; <sup>3</sup>Department of Otolaryngology, Bern University Hospital, Inselspital, University of Bern, Switzerland; <sup>4</sup>Department of Oral and Maxillofacial Surgery, University Hospital Heidelberg, Germany; <sup>5</sup>Department of Neuroradiology, University Hospital Heidelberg, Germany Q4 Q5 Q6

*K. Zaoui, A. Jung, W. Wimmer, M. Engel, M.A. Möhlenbruch, P.A. Federspil: Topographic bone thickness maps to evaluate the intuitive placement of titanium miniplates for nasal prostheses. Int. J. Oral Maxillofac. Surg.* 2019; xxx: xxx–xxx. © 2020 International Association of Oral and Maxillofacial Surgeons. Published by Elsevier Ltd. All rights reserved.

**Abstract.** The aim of this study was to evaluate the intuitive placement of titanium miniplates. The hypothesis was that virtual planning can improve miniplate placement. Twenty patients were included in the study. These patients were fitted with 21 titanium miniplates (16 y-plates, three t-plates, and two u-plates) to retain nasal prostheses between 2005 and 2017. Colour-coded topographic bone thickness maps (TBTMs) were created in fused pre- and postoperative computed tomography. Implants were virtually transposed at the position of highest bone thickness. The bone thickness index (BTI) was calculated as the sum of points assigned at each screw (1 point per millimetre up to 4 mm, and 5 points for greater values) divided by the number of screws. One plate broke after 2.8 years, thus plate survival after 5 years was 91% using the Kaplan–Meier method. The BTI for all 21 plates increased from 3.4 to 4.1 points using virtual transposition ( $P < 0.001$ ). No significant changes were observed in t- and u-plates, but the median BTI increased from 3.1 to 4.1 points ( $P < 0.0005$ ) in 16 y-plates. The change was substantial ( $\geq 0.5$  points) in 9/16 y-plates. Therefore, the hypothesis that virtual planning improves implant placement was accepted.

**Key words:** bone plates; bone-anchored prosthesis; computer-assisted surgery; maxillofacial prosthesis implantation; titanium.

Accepted for publication 26 February 2020

Q8 Nasal prostheses can be retained by inserting screw-shaped extraoral implants into the glabella or floor of the nose<sup>1,2</sup>. However, the placement of these Brånemark-type implants can be difficult because the bone stock is low at the piriform aperture<sup>3,4</sup>. In a case report, Proussaefs

suggested using the frontal process of the maxilla together with other implantation areas. Alternatively, long zygoma implants may be used<sup>6,7</sup>. In the 1990s, Farmand developed the Epitec system, which consisted of a titanium grid, but this is no longer marketed<sup>8</sup>. In our centre,

Epiplating system titanium plates (Medicon eG, Tuttlingen, Germany) are used (Fig. 1). They allow forces to spread on multiple 2.0 bone screws to promote implant stability<sup>3</sup>. These plates have various geometries (Figs 1,3,6) and are easy to adapt to the bone surface without Q9 Q10

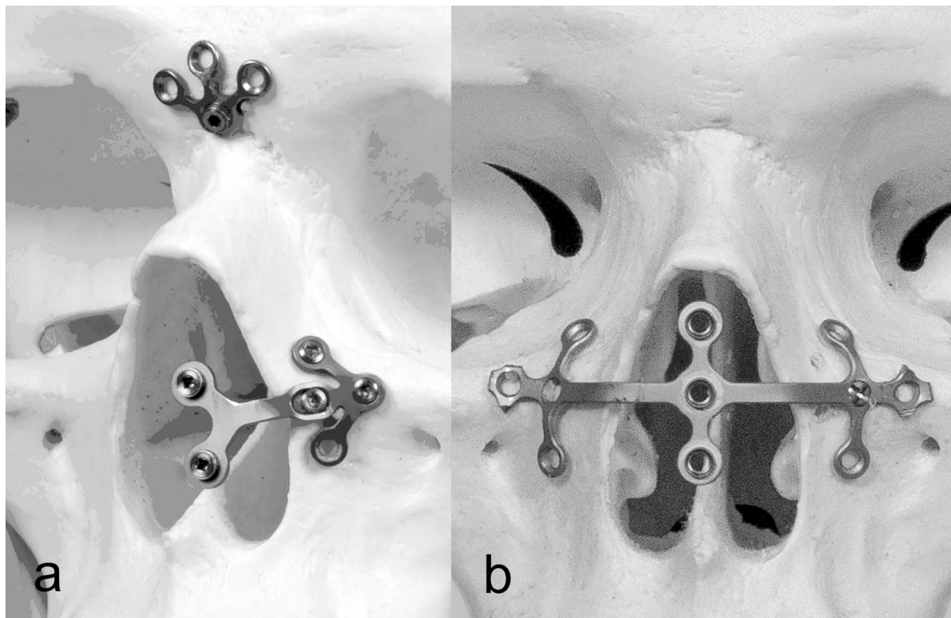


Fig. 1. Schematic drawing of the titanium miniplates used for retention of craniofacial prostheses (Epiplating system by Medicon eG, Tuttlingen, Germany). (A) Below, a y-plate is placed at the lateral aspect of the piriform aperture. Above, a u-plate is inserted at the glabella using three of six possible arms. Note this position is only used if the nasal bones are removed. (B) A t-plate bridges the nasal cavity.

preoperative computer-aided surgical planning<sup>3,9–11</sup> (Figs 4 and 5).

The aim of this study was to evaluate intuitive implant placement. The hypothesis was that virtual planning improves the placement of Epiplating titanium plates at areas of higher bone stock. Several studies have assessed the spatial and angular accuracy of implant placement<sup>12–22</sup>, but this requires reference to an existing surgical plan and is not appropriate for assessing intuitively placed implants. Therefore, a method of evaluating implant placement was developed using a scoring system based on the underlying bone thickness, without reference to a surgical plan. The topographic bone thickness map (TBTM) was a useful tool for three-dimensional colour-coded representation of bone thickness, as shown in Figs 2 and 6<sup>23</sup>. TBTMs have been used at the ARTORG Center for Biomedical Engineering Research, University of Bern, Switzerland to plan the placement of bone-anchored vascular access ports<sup>23</sup> and to judge the spatial constraints of hearing implants in the mastoid cavity<sup>24</sup>. Creating a TBTM for temporal bone can be time-consuming because mastoid air cells often impede automatic bone segmentation. As this is much less problematic in the midface, an automated TBTM output was applied after preliminary bone segmentation using Amira software (Thermo Fisher Scientific – Fei, Hillsboro, OR, USA). This study evaluates

the use of TBTMs to visualize bone stock in the midface and to evaluate the intuitive placement of extraoral implants based on underlying bone thickness.

### Materials and methods

The study included patients fitted with intuitively placed titanium implants to retain nasal prostheses from 1 January 2005 to 13 June 2017. Inclusion criteria were a preoperative and a postoperative CT scan and follow-up information on implant survival. Exclusion criteria were patient records without a preoperative and a postoperative CT scan and follow-up information on implant survival. No patient underwent radiographic imaging purely for this study. Out of 42 patients receiving implants during this period, 20 fulfilled all the inclusion criteria and were included in the study. The local Ethics Committee approved the study (S-512/2016). The study was reported in compliance with the EQUATOR guidelines for observational studies (STROBE).

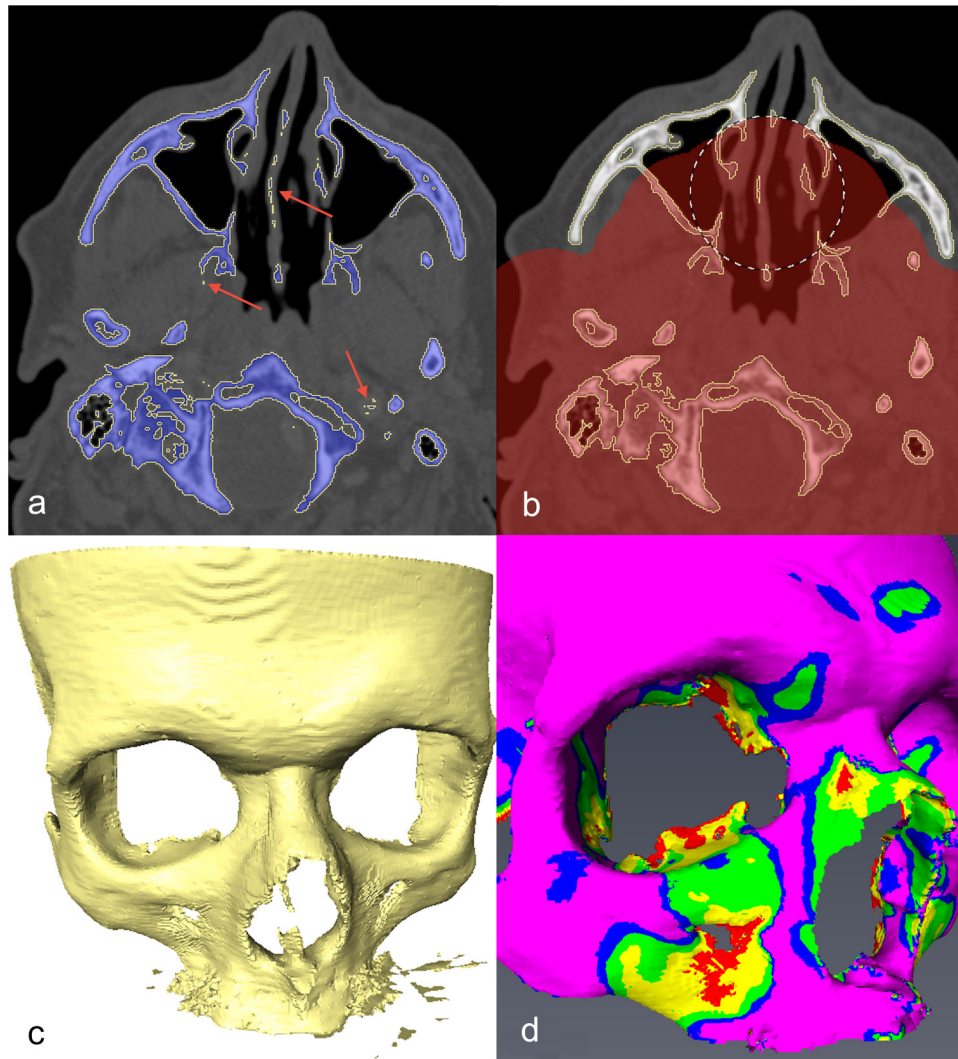
### Patient characteristics and implants

The mean age at the time of implantation was 64.9 (standard deviation: 9.1) years (range: 52–81.8 years). The mean age of five female patients was 60.3 years, and the mean age of 15 male patients was 66.4

years. Neoplastic disease was the reason for rhinectomy in all patients.

Twelve patients had radiotherapy at the implant region with an average dosage of 65.2 Gy. Radiotherapy was concomitant with chemotherapy in three patients. Radiotherapy was delivered after implantation in 10 cases, and before implantation in two cases.

The patients were followed up at regular intervals to exclude progressive disease. Clinical examinations with nasal endoscopy were performed, and implant stability was checked manually. Follow-up data were collected by chart review. The median follow-up duration was 3.2 years (mean: 3.5 years), with a range of 0.5–11.6 years. All patients were fitted with Epiplating system titanium implants (Medicon eG, Tuttlingen, Germany). The Epiplating system is CE-marked for extraoral bone-anchorage of craniofacial prostheses. Three types of Epiplating implants (Figs 1,3 and 6) were used: (1) the y-shaped nasal plate ('y-plate'), which is inserted unilaterally with a maximum of four screws; (2) the transversal nasal plate ('t-plate'), which is fixed on both sides of the nasal defect with up to nine screws on either side; and (3) the star-shaped universal plate ('u-plate'), which is fixed with up to six bone screws. The 20 included patients were fitted with 21 implants in total (16 y-plates, three t-plates, and two u-plates), and a total of



**Q1** Fig. 2. (A) Bone segmentation (blue) in preoperative computed tomography data. Red arrows point to excluded small islands of bone-equivalent density, e.g., calcification in blood vessels. (B) The region of interest is confined to the midfacial skeleton; the circled and red painted areas are excluded. (C) Oblique view of the three-dimensional representation of the area of interest. Note that the deeper bony structures are removed, as they would interfere with visual interpretation. (D) The segmented skull is shown with the topographic bone thickness map (TBTM). Bone thickness is colour-coded as follows: 0–1 mm = red, 1–2 mm = yellow, 2–3 mm = green, 3–4 mm = blue, and >4 mm = violet. (For interpretation of the references to colour in the figure legend and text, the reader is referred to the web version of this article.)

129 bone screws were used to fix the plates.

#### Surgical procedure

Implants were fixed to the frontal process of the maxillary bone on the lateral aspect of the piriform aperture at the level of the infraorbital rim (Figs 1,3). The senior author performed the implant surgery. The implants were placed intuitively without any navigational systems or pre-planned drilling templates. Intraoperatively, the implants were bent to fit the bony contour at the implantation site. Cover screws temporarily secured the threads for magnets during the bending

procedure to prevent unwanted distortion. The implants were fixed with self-tapping titanium bone screws (2.0 osteosynthesis system), usually 4 or 5.5 mm long. The skin penetration site with these Epiplating nasal implants is only a small area around the backbone of the plate. The implants were left unloaded for 6 weeks in non-irradiated patients, and for 6 months after radiotherapy. There was no need for second-stage surgery as the threaded holes were already inside the nasal cavity.

#### CT data analysis with TBTM

CT data were imported in the DICOM visualizing and analyzing software pack-

age Amira Version 6.4.0 (Thermo Fisher Scientific – Fei, Hillsboro, OR, USA). The ortho slice function was used to visualize the DICOM data. The crop editor eliminated mobile structures outside the region of interest (ROI), and the data window was set to bone levels. The bone within the ROI was segmented using thresholding. Contrast medium within vessels was excluded using the ‘remove islands’ function (Fig. 2A). All parts of the skull lying deep to the paranasal region were manually excluded using the brush function (Fig. 2B). After that, the segmented paranasal bone was visualized by the surface view function (Fig. 2C). A TBTM was generated from preoperative CT data

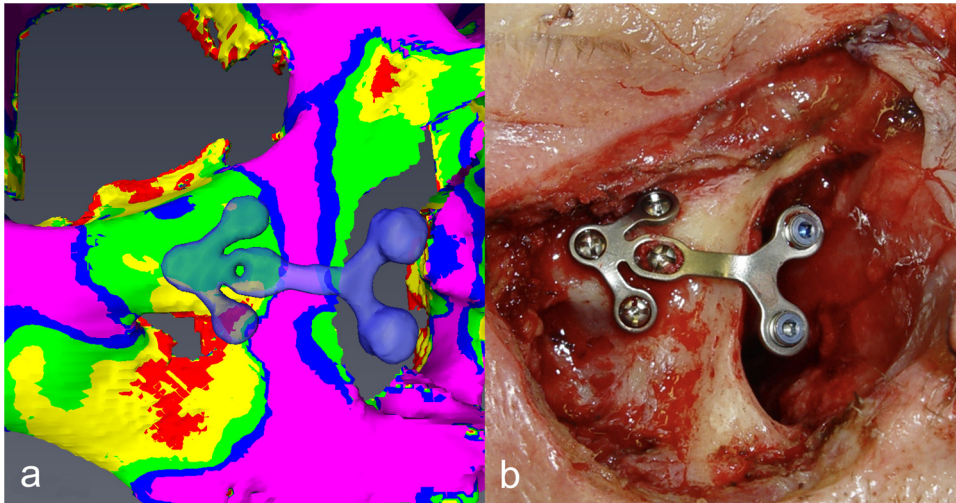


*Fig. 3.* (A) Topographic bone thickness map (TMTM) of the preoperative computed tomograph fused with the implant representation (y-plate) in the postoperative data set. (B) The corresponding intraoperative photograph of the inserted y-plate on the frontal process of the maxilla. The two threaded holes of the plate lying inside the nasal cavity are temporarily secured with blue cover screws until definitive loading. (For interpretation of the references to colour in the figure legend and text, the reader is referred to the web version of this article.)

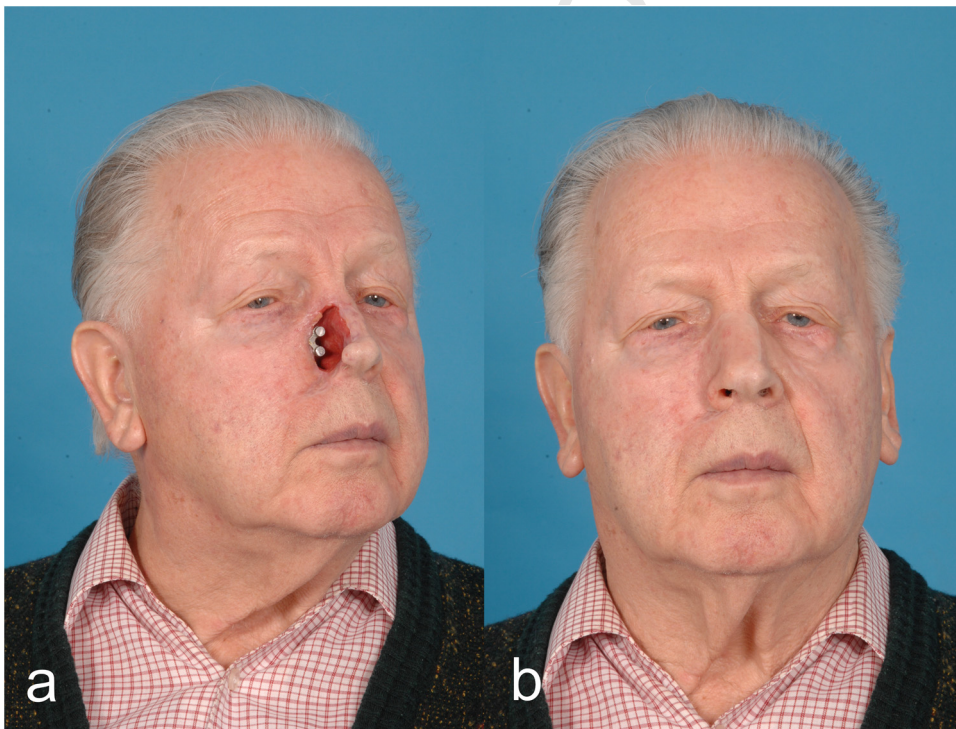


*Fig. 4.* (A) Postoperative photograph of the patient shown in Figs 1 and 2. The plate is loaded with two magnets. (B) The patient with the implant-retained nasal prosthesis (anaplastologist: Jörn Brom, Heidelberg).

using the ‘surface thickness’ module with colour-coding perpendicular to each surface point (Fig. 2D). The algorithm was previously described by Guignard et al.<sup>23</sup>. Bone thickness was colour-coded as follows: 0–1 mm = red, 1–2 mm = yellow, 2–3 mm = green, 3–4 mm = blue, and >4 mm = violet. It took approximately

10 min for a trained user to process the TBTM.

#### **Bone thickness score and bone thickness index**

The y-plates had four distinct bone screw positions: cranial, caudal, medial, and lat-

eral (Fig. 3). There was an additional screw location (median) for the t-plates. The u-plates were placed centrally, thus the screw positions were left, right, and middle. For each bone screw site, a score was assigned based on the bone thickness: 0–1 mm = 1 point, 1–2 mm = 2 points, 2–3 mm = 3 points, 3–4 mm = 4 points, and

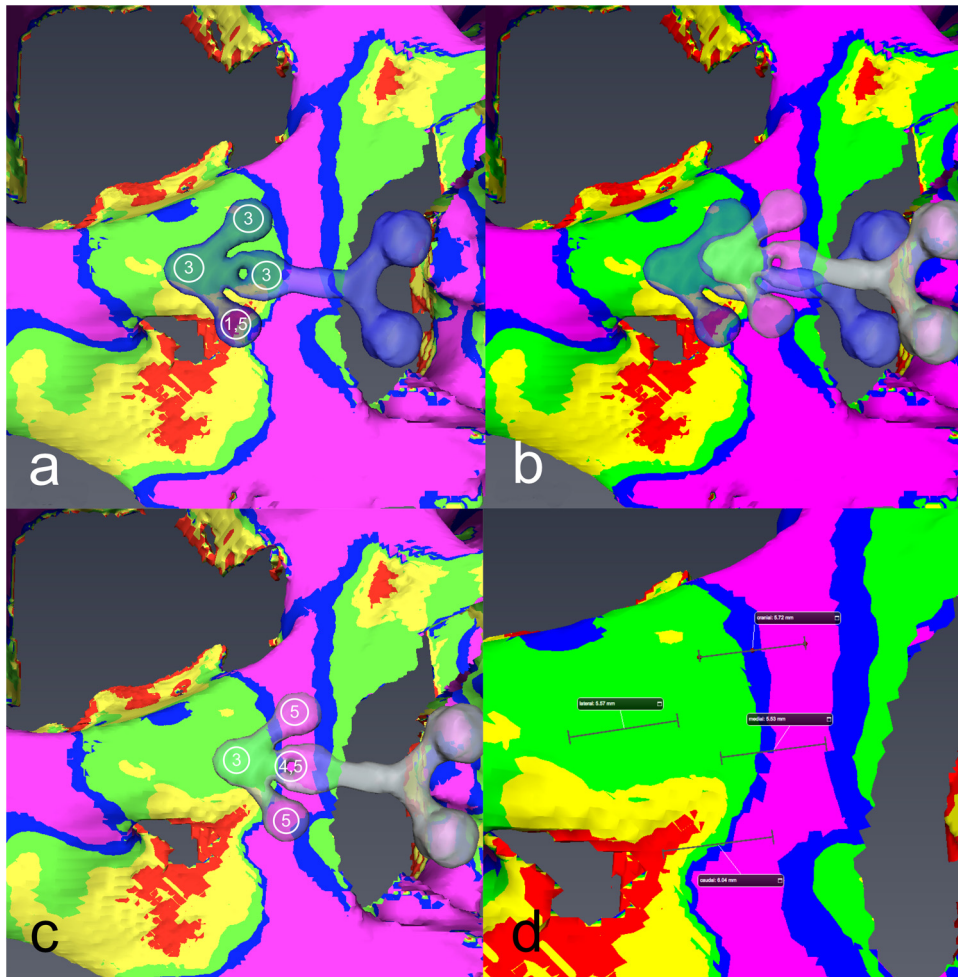


*Fig. 5.* (A) The original position of the plate is shown in light blue. The four bone screw positions were cranial, caudal, medial and lateral. The score points for each bone screw are depicted in white circles. The bone thickness score (BTS) is 10.5, and the bone thickness index (BTI) is 2.6. (B) The virtually transposed plate is shown in light grey. (C) Points depict the transposed position. Here, the BTS is 17.5, and the BTI is 4.4. (D) The vectors for the transposition are shown for each bone screw. The average length is 5.2 mm, which represents the second-longest vector of all transpositions. (For interpretation of the references to colour in the figure legend, the reader is referred to the web version of this article.)

>4 mm = 5 points (Fig. 5A). In cases of ambiguity, when a borderline between two categories was running through the area of a burr hole, half a point was added to the lower value. The total points at each screw position gave the bone thickness score (BTS) for the implant, and the BTS was divided by the number of bone screws to give the bone thickness index (BTI) for the implant. The BTI is equivalent to the average score per bone screw position and is independent of the number of bone screws used in an individual plate, so it can be used to compare plates with different numbers of fixation screws. The possible BTI range was 1–5 points (the minimum and maximum scores per bone screw).

#### Virtual implant transposition

The ‘register images’ module allowed the pre- and postoperative data (‘co-registra-

tion’) to be fused. The correctness of image fusion was verified in all geometric planes. The implant plate was segmented and colour-coded in light blue (Fig. 3). As a virtual object, the implant was duplicated and colour-coded in light grey (Fig. 5B, C). The duplicated object was then virtually transposed using the ‘transform editor’ with the superimposed TBTM indicating the region of greatest bone thickness (judged by the senior author), as would have been carried out in preoperative planning. Every effort was made to sit the plate flat on the new bony surface position in all three dimensions. However, the shape of the plate could not be changed in the software, thus the implant could not be positioned as well as it could during surgery. Because of this, each side of the t-plate had to be transposed separately. The BTI of the original was compared with that of the virtually transposed position.

An increase in BTI of 0.5 points or more was considered substantial and clinically relevant; anything less was deemed to be a marginal improvement. The length of the transposition vector was measured in millimetres for each bone screw, and an average was calculated for the whole implant (Fig. 5D).

#### Statistical analysis

Data were analysed with the software package IBM SPSS Statistics for Windows, version 24.0 (IBM Corp., Armonk, NY, USA). The Shapiro–Wilk test was used to check for normal distribution. Student’s *t*-test for paired samples was used to check differences between means. If the data were not normally distributed, the Wilcoxon test was used. A *P*-value <0.05 was considered statistically significant. The Kaplan–Meier method was used

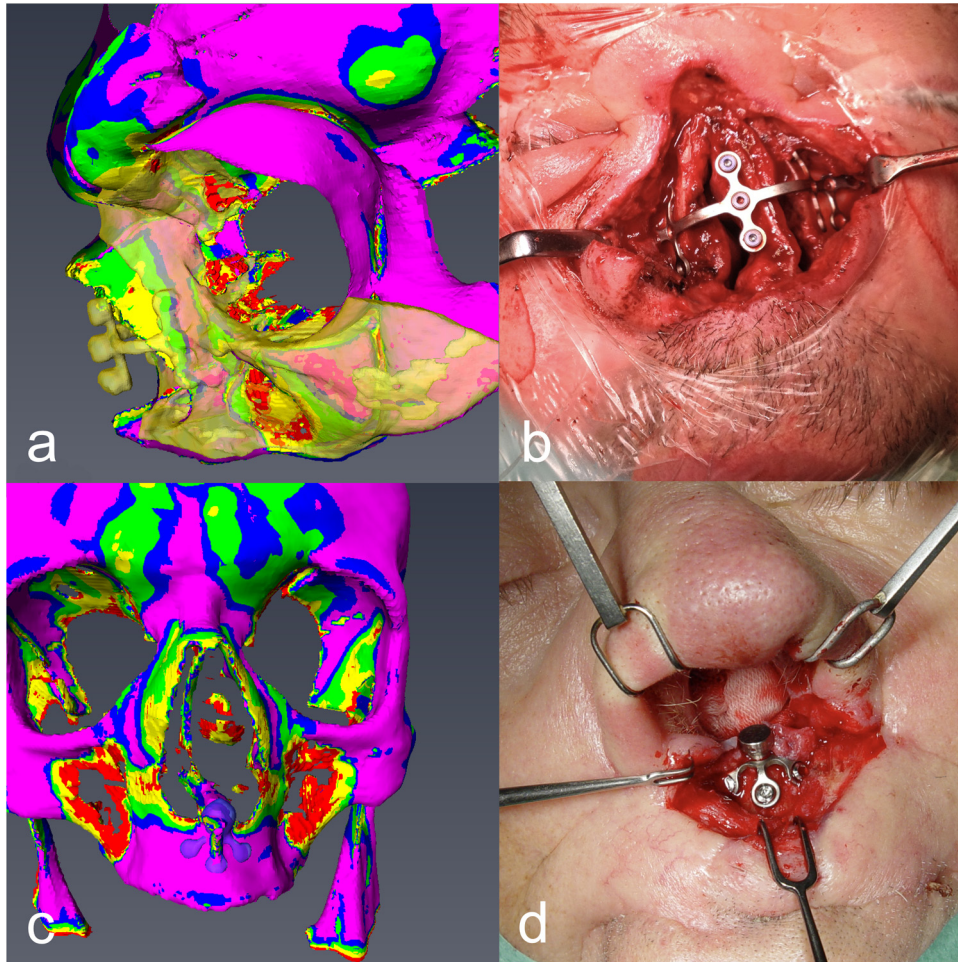


*Fig. 6.* (A) A topographic bone thickness map (TBTM) for a patient with a transverse miniplate (t-plate) fixed on both sides of the piriform aperture. (B) The corresponding intraoperative photography. (C) A TBTM for a patient with a universal miniplate (u-plate) at the premaxilla. (D) The corresponding intraoperative photography.

to calculate the time-dependent plate survival rate over time from incomplete observations.

## Results

Twenty-one plates were fixed with a total of 129 bone screws. The BTS for all plates ranged from 7 to 20.5 points, with an average of 13.7 points ( $\pm 3.99$ ). Virtual transposition improved the BTS to an average of 16.5 points ( $\pm 2.81$ ), ranging from 11 to 23 points. The BTI increased from 3.4 to 4.1 points, and this difference was statistically significant ( $P < 0.001$ ). The vector of transposition for all plates ranged from 0 to 6.8 mm, with a median of 2.37 mm and an average of 2.42 mm. The TBTM showed that bone stock is highest along the pillar of the frontal process of the maxilla (Figs 2,6). This finding was consistent across individual specimens. Bone thickness was lowest at the frontal wall of the antrum. Bone thickness at the infra-

orbital rim was intermediate and less consistent between individuals.

### Osseointegration and plate survival

All the implants osseointegrated successfully and remained so during follow-up. One y-plate broke after 2.8 years at the level of the oval (medial) screw hole, but bone grew over all bone screws and the remaining part of this plate. The reason for this break was not clear. Including the broken plate, plate loss was 1/21 (4.8%). The estimated time-dependent survival rate for the titanium plates was 91% after 3 and 5 years, according to the Kaplan–Meier method. None of the 129 bone screws were lost, but four were deliberately removed with the broken plate.

### y-Plates

The 16 y-plates were fixed with 96 bone screws altogether. The BTS ranged from 7

to 18 points per implant with an average of 12.4 points. Each y-plate was fixed with four bone screws, thus the BTI ranged from 1.75 to 4.5 points with a median of 3.1 points (mean: 3.1 points). Virtual implant transposition improved the BTS for the y-plates by 3.7 points to an average 16.1 points. This translates to a median BTI improvement of 4.1 points (mean: 4.0 points). The difference was statistically significant ( $P < 0.0005$ ). Regarding changes at distinct screw positions (Fig. 8), the median BTI improved the most at the caudal position (from 3.2 points to 5.0 points;  $P = 0.001$ ), and improved the least at the lateral position (from 2.5 points to 2.7 points;  $P = 0.17$ ). The median BTI values changed from 3.5 to 5.0 points at the cranial position, and from 3.0 to 4.5 points at the medial position. The change was substantial ( $\geq 0.5$  BTI points) in nine (56%) of 16 cases. There was no change in BTI in two cases (12.5%), and a marginal difference in five

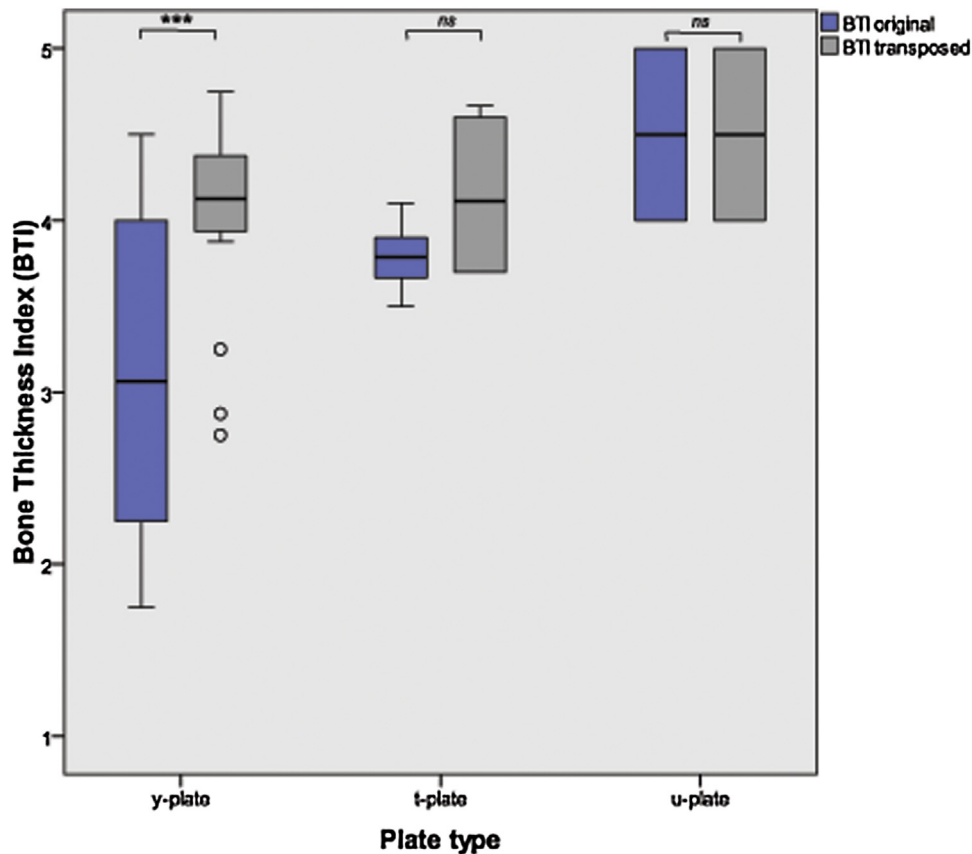


Fig. 7. Box plots of the bone thickness index (BTI) at the original (blue) and the transposed (grey) position stratified by plate subtype. Significance levels are given above the boxes. (For interpretation of the references to colour in the figure legend, the reader is referred to the web version of this article.)

(31%) cases. The BTS decreased at one screw position in four (25%) of the 16 transpositions, but improved at the other three screw positions. The vector for transposing the y-plates ranged from 0 to 6.8 mm (median: 2.4 mm, mean: 2.7 mm).

#### t- Plates

The three t-plates were retained by a total of 27 bone screws. The BTS ranged from 26.5 to 39 points with an average of 34.2 points for the whole implant. The median BTI for t-plates was 3.8 points. The median BTI for each side of the t-plates improved by 0.3 points to 4.1 points after virtual transposition (Fig. 7), but this difference was not significant ( $P = 0.068$ ). In one-third of cases the change was substantial, in another third of cases there was no change, and in the final third of cases, the difference was marginal. The vector for the transposition at each side ranged from 0 to 4.8 mm (mean: 2.4 mm, median: 3.3 mm).

#### u- Plates

The two u-plates were fixed with a total of six bone screws (three bone screws each).

The BTS ranged from 13 to 15 points, with an average of 13.5 points per implant. The median BTI for u-plates was 4.5 points (Fig. 7). The BTS was not improved by transposition, thus the vector length was 0 mm.

#### Discussion

In a recent meta-analysis, Chrcancovic et al.<sup>25</sup> found significantly higher implant failure rates for craniofacial implants retaining nasal (12.2%) and orbital prostheses (12.1%) than for auricular prostheses (1.2%). Reduced implant survival in the paranasal regions may be explained by the relatively low bone stock in this area. In this study, bone thickness was highest at the frontal process of the maxilla, the glabella, and the premaxilla. The infraorbital rim offers the least bone stock, as shown in Figs 2 and 6.

Several studies have investigated the quality of the actual implant position compared with a pre-planned position<sup>12–22</sup>. For computer-aided implant placement, either static methods with templates or dynamic systems with intraoperative navigation can be used. Van Assche et al.<sup>19</sup>

performed a meta-analysis on the accuracy of computer-aided dental implant placement. The mean error was approximately 1.0 mm (range: 0–6.5 mm) at the entry point and 1.24 mm (range: 0–6.9 mm) at the implant apex. The mean angular deviation was 3.8° (range: 0–24.9°). Preoperative computer-based planning is also possible for extraoral dental-type implants<sup>26,27</sup>. However, the accuracy of dental implant placement is likely higher than for extraoral implants. Dings et al.<sup>13</sup> conducted a cadaver study to evaluate the accuracy of guided implant placement in the orbital, nasal, and auricular regions using computer-aided designed stereolithographic skin-supported surgical templates with and without bone fixation pins. The mean deviation was 3.3 mm with pins and 2.5 mm without pins, and the mean angulation error was 8° with pins and 6° without pins. The accuracy of implant placement varied depending on the anatomic region and was highest at the auricle. Surprisingly, surgical templates with bone fixation pins produced more implant deviations than non-fixed surgical templates. Ciocca et al.<sup>21</sup> reported computer-aided design and manufacturing (CAD-

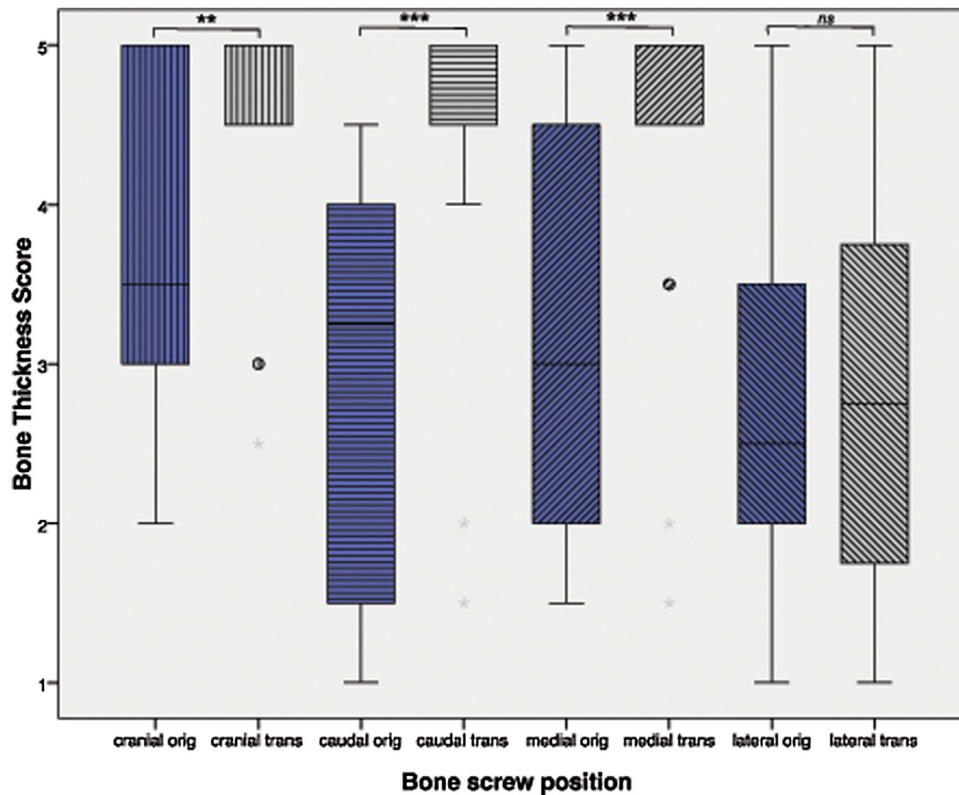


Fig. 8. Box plots of the bone thickness score (BTS) for specific bone screw positions at the original (blue) and the transposed (grey) position. Significance levels are given above the boxes. (For interpretation of the references to colour in the figure legend, the reader is referred to the web version of this article.)

CAM) construction of a surgical template for placing a nasal prosthesis with a deviation from the plan between 1.2 and 3.4 mm.

The above-cited studies compared the accuracy of intraoperative implant placement based on a predetermined plan, but not the quality of the planning itself with regards to underlying bone thickness. Furthermore, these studies only evaluated pre-planned implants, not intuitively placed fixtures. We are not aware of any study that has investigated intuitive, unplanned implant placement. To address this, we present a method of evaluating intuitive implant placement using TBTM. Using co-registration, the titanium plate was visualized on the postoperative CT scan superimposed on the TBTM, which was derived from preoperative data. Artifacts from the implant metal precluded the use of a single postoperative CT.

To evaluate implant placement in terms of underlying bone thickness, we introduced a 1- to 5-point scoring method at each site of bone screw fixation. Scores were compiled from all screw positions to give the BTS for each implant. However, because different implant geometries were

fixed with diverging numbers of bone screws, the BTI (the BTS divided by the number of used screws) is a more relevant value, and was used to compare different plate types. The two u-plates had the highest median BTI (4.5 points) (Fig. 7), and were placed in the glabella and the premaxilla (Fig. 6). The t-plates had the second highest BTI (3.8 points) followed by the y-plates (3.1 points) (Fig. 7).

To see whether implant placement can be optimized based on bone thickness at the area of bone screw insertion, the implant was virtually transposed as a segmented object using Amira software. The aim was to augment the BTI, but improvement in one screw position might be detrimental to another screw position. This happened in one out of four transpositions. Interestingly, the BTI values of u-plates and t-plates were not improved by transposition. However, the mean BTI of y-plates increased significantly from 3.1 to 4.02 points (Fig. 7). This translates to approximately 1 mm more bone at every screw position, which was considered clinically relevant. Interestingly, the BTI improved significantly at all screw positions except the lateral position (Fig. 8).

This position is located at the infraorbital rim, which had the lowest BTS. Slight imprecisions in this region may direct the bone screw towards the very thin frontal wall of the antrum. However, not every transposition improved the BTI substantially (i.e. by at least 0.5 points). Although the BTI increased substantially in only half of the y-plates, the remaining half were still well placed by the intuitive method. Whether improved implant placement at regions of higher bone thickness is clinically relevant remains unclear, as none of the plates in this cohort lost osseointegration. However, implant losses have been reported for the plate system. Sandner and Bloching<sup>11</sup> reported an implant survival rate of 82% in a small series of nine patients fitted with y-shaped plates, and Papispyrou et al.<sup>10</sup> a survival rate of 90% in 22 patients fitted with y-shaped plates. Lünenbürger et al.<sup>9</sup> found a 96% survival rate of 53 implants fitted with transverse plates.

The transposed ideal position was very close to the original position, as demonstrated by the median length of the vector (2.4 mm for y-plates). None the less, this study advocates preoperative planning

based on bone thickness. It remains to be seen whether implants can be placed with sufficient accuracy intraoperatively. The accuracy of implant placement may be improved using a colour-coded 3D print of CT data with the TBTM. This would allow the surgeon to pre-bend the plate according to the anatomy and underlying bone thickness. However, the export function for printable colour-coded stl-files in Amira needs further development. Software solutions to these problems are rapidly evolving.

A limitation of the study was that the transposed implant as a virtual object could not be bent to exactly fit the new surface area. While this was not critical for y- and u-plates, the t-plates needed to be adapted to the bone on the opposite side. Therefore, t-plates were analysed separately on each side. Furthermore, we could not control the magnets' location of the transposed implant position to promote anaplastologic usefulness and to avoid collision with the cartilaginous septum. The plate may need to be bent to achieve this control. The good results of intuitive plate placement observed in this study might be a consequence of the senior author's experience, and may not be easily reproducible. However, the authors believe that these plates are easier to place than conventional osseointegrated titanium implants.

A strength of the study is the methodology with TBTM, which can evaluate the actual implant position without previous computer-based planning. This method is not limited to unplanned implants and could be used to analyse pre-planned implants and their optimal placement based on bone thickness.

In conclusion, TMTMs are a useful tool for evaluating implant placement based on underlying bone thickness. Bone thickness was highest at the frontal process of the maxilla, the glabella, and the premaxilla, and was lowest at the frontal wall of the antrum. Bone thickness at the infraorbital rim was intermediate and less consistent between individuals. All u-plates and t-plates, and 44% of y-plates were placed in the positions of optimal bone thickness using the intuitive method. Half of the y-plates could have been implanted on substantially higher bone stock but were still close (median: 2.4 mm) to the optimal positions. Therefore, the hypothesis that virtual planning improves placement was accepted. Ideally, planning would control for bone thickness at the designated region, and identify areas of very low bone thickness. Moreover, planning software for the placement of plates needs to allow

virtual bending of the plates to optimize both the fitting of the plate to the bone and the location of the magnets for prosthetic needs. While some software can do this by manual adjustment, no ready-to-use planning software is available for the plates yet. Furthermore, it remains to be seen whether implants can be placed within the millimetre range intraoperatively.

### Funding

This study was not funded.

### Competing interests

K.Z. has received payment for conference travel expenses from Medicon eG (Tutlingen, Germany).

### Ethical approval

The study was conducted in accordance with the ethical standards of the 1964 Declaration of Helsinki and its later amendments. The Ethics Committee of the University of Heidelberg Medical Faculty approved the study (S-512/2016).

### Patient consent

Written patient consent was obtained.

**Acknowledgments.** The authors thank Claire Bacon, PhD, for language editing of the manuscript.

### References

- Ethunandan M, Downie I, Flood T. Implant-retained nasal prosthesis for reconstruction of large rhinectomy defects: the Salisbury experience. *Int J Oral Maxillofac Surg* 2010;**39**:343–9.
- Korfage A, Raghoebar GM, Noorda WD, et al. Recommendations for implant-retained nasal prostheses after ablative tumor surgery: minimal surgical aftercare, high implant survival, and satisfied patients. *Head Neck* 2016;**38** Suppl 1:E619–24.
- Federspil PA. Implant-retained craniofacial prostheses for facial defects. *GMS Curr Top Otorhinolaryngol Head Neck Surg* 2009;**8**:Doc03.
- Thiele OC, Brom J, Dunsche A, et al. The current state of facial prosthetics — a multicenter analysis. *J Craniomaxillofac Surg* 2015;**43**:1038–41.
- Proussaefs P. Use of the frontal process of the maxillary bone for implant placement to retain a nasal prosthesis: a clinical report. *Int J Oral Maxillofac Implants* 2004;**19**:901–5.
- Scott N, Kittur MA, Evans PL, Dovgalski L, Hodder SC. The use of zygomatic implants for the retention of nasal prosthesis following rhinectomy: the Morriston experience. *Int J Oral Maxillofac Surg* 2016;**45**:1044–8.
- Dawood A, Kalavresos N. Management of extraoral complications in a patient treated with four zygomatic implants. *Int J Oral Maxillofac Implants* 2017;**32**:893–6.
- Farmand M. [A new implant system for the fixation of facial prostheses] in German. *Dtsch Z Mund Kiefer Gesichtschir* 1991;**15**:421–7.
- Lunenburger H, Roknic N, Klein M, Wermker K. Treatment outcome of the transfacial titanium epiplating system for total nasal defects. *Plast Reconstr Surg* 2016;**137**:405e–13e. Q12
- Papaspyrou G, Schick B, Schneider M, Al Kadah B. Epithetic nasal reconstruction for nasal carcinoma: retrospective analysis on 22 patients. *Eur Arch Otorhinolaryngol* 2017;**274**:867–72.
- Sandner A, Bloching M. Retrospective analysis of titanium plate-retained prostheses placed after total rhinectomy. *Int J Oral Maxillofac Implants* 2009;**24**:118–23.
- Alharethy S, Alohalı S, Alquniabut I, Jang YJ. Bone and soft tissue nasal angles discrepancies and overlying skin thickness: a computed tomography study. *Aesthetic Plast Surg* 2018;**42**:1085–9.
- Dings JPJ, Verhamme L, Maal TJJ, Merckx MAW, Meijer GJ. Reliability and accuracy of skin-supported surgical templates for computer-planned craniofacial implant placement, a comparison between surgical templates: with and without bony fixation. *J Craniomaxillofac Surg* 2019;**47**:977–83. Q13
- Dreiseidler T, Neugebauer J, Ritter L, et al. Accuracy of a newly developed integrated system for dental implant planning. *Clin Oral Implants Res* 2009;**20**:1191–9.
- Gillot L, Cannas B, Friberg B, et al. Accuracy of virtually planned and conventionally placed implants in edentulous cadaver maxillae and mandibles: a preliminary report. *J Prosthet Dent* 2014;**112**:798–804.
- Pettersson A, Kero T, Gillot L, et al. Accuracy of CAD/CAM-guided surgical template implant surgery on human cadavers: part I. *J Prosthet Dent* 2010;**103**:334–42. Q14
- Pettersson A, Kero T, Soderberg R, Nasstrom K. Accuracy of virtually planned and CAD/CAM-guided implant surgery on plastic models. *J Prosthet Dent* 2014;**112**:1472–8.
- Ruckschloss T, Ristow O, Muller M, Kühle R, Zingler S, Engel M, Hoffmann J, Freudlsperger C. Accuracy of patient-specific implants and additive-manufactured surgical splints in orthognathic surgery — a three-dimensional retrospective study. *J Craniomaxillofac Surg* 2019;**47**:847–53.
- Van Assche N, Verbruyssens M, Coucke W, et al. Accuracy of computer-aided implant

- placement. *Clin Oral Implants Res* 2012;**23** Suppl 6:112–23.
20. Zhou W, Liu Z, Song L, Kuo CL, Shafer DM. Clinical factors affecting the accuracy of guided implant surgery — a systematic review and meta-analysis. *J Evid Based Dent Pract* 2018;**18**:28–40.
21. Ciocca L, Fantini M, De Crescenzo F, Persiani F, Scotti R. Computer-aided design and manufacturing construction of a surgical template for craniofacial implant positioning to support a definitive nasal prosthesis. *Clin Oral Implants Res* 2011;**22**:850–6.
22. Vasak C, Watzak G, Gahleitner A, et al. Computed tomography-based evaluation of template (NobelGuide)-guided implant positions: a prospective radiological study. *Clin Oral Implants Res* 2011;**22**:1157–63.
23. Guignard J, Arnold A, Weisstanner C, Caversaccio M, Stieger C. A bone-thickness map as a guide for bone-anchored port implantation surgery in the temporal bone. *Materials (Basel)* 2013;**6**:5291–301.
24. Wimmer W, Gerber N, Guignard J, et al. Topographic bone thickness maps for Bone-bridge implantations. *Eur Arch Otorhinolaryngol* 2015;**272**:1651–8.
25. Chrcanovic BR, Nilsson J, Thor A. Survival and complications of implants to support craniofacial prosthesis: a systematic review. *J Craniomaxillofac Surg* 2016;**44**:1536–52.
26. McHutchion L, Kincade C, Wolfaardt J. Integration of digital technology in the workflow for an osseointegrated implant-retained nasal prosthesis: a clinical report. *J Prosthet Dent* 2019;**121**:858–62.
27. Buzayan MM, Yunus NB, Oon HK, Tawfiq O. Virtual treatment planning for implant-retained nasal prosthesis: a clinical report. *Int J Oral Maxillofac Implants* 2017;**32**:e255–8.

## Address:

Philippe A. Federspil  
Division of Oncological ORL Surgery  
Department of Otorhinolaryngology  
Heidelberg University Hospital  
Im Neuenheimer Feld 400/69120  
Heidelberg  
Germany  
Tel.: +49 6221 566705  
Fax: +49 6221 5633637  
E-mail: [federspil@med.uni-heidelberg.de](mailto:federspil@med.uni-heidelberg.de)